Design of coupling for synchronization of chaotic oscillators

Ioan Grosu,[1] Ranjib Banerjee,[2] Prodyot K. Roy,[3] and Syamal K. Dana[2]
[1]*Faculty of Bioengineering, University of Medicine and Pharmacy "Gr. T. Popa," Iasi, 700115 Romania*
[2]*Central Instrumentation, Indian Institute of Chemical Biology (Council of Scientific and Industrial Research), Kolkata 700032, India*
[3]*Department of Physics, Presidency College, Kolkata 700073, India*
(Received 30 December 2008; published 23 July 2009)

A general procedure is discussed to formulate a coupling function capable of targeting desired responses such as synchronization, antisynchronization, and amplitude death in identical as well as mismatched chaotic oscillators. The coupling function is derived for unidirectional, mutual, and matrix type coupling. The matrix coupling, particularly, is able to induce synchronization, antisynchronization, and amplitude death simultaneously in different state variables of a response system. The applicability of the coupling is demonstrated in spiking-bursting Hindmarsh-Rose neuron model, Rössler oscillator, Lorenz system, Sprott system, and a double scroll system. We also report a scaling law that defines a process of transition to synchronization.

DOI: 10.1103/PhysRevE.80.016212 PACS number(s): 05.45.Xt, 05.45.Gg

I. INTRODUCTION

The concept of synchronization [1] in dynamical systems is able to explain collective behaviors of oscillatory systems and many spatial patterns observed in nature and artificial systems. These observations usher in potential applications in complex living systems [2,3] such as heart and brain and in engineering systems such as secure communication [4] and weak magnetic field sensing [5]. From the viewpoint of applications, control of synchronization and ability to engineer such coherent behaviors in dynamical systems are important. Control of synchronization as well as desynchronization [6,7] is, particularly, important in relevance to brain dynamics. An automatic control of phase synchronization (PS) in coupled oscillators was proposed earlier [8] for applications in engineering, ecology, and medicine. Recently, engineering [9] desired responses such as sequential patterns as well as desynchronization is explored in a population of oscillators using feedback control. Formulating appropriate coupling function in dynamical systems can be an important approach for realizing and controlling desired coherent behaviors such as complete synchronization (CS) [10], antisynchronization (AS) [11], lag synchronization (LS) or PS [12], generalized synchronization [13], and time-scale synchronization [14]. Besides synchronized states in coupled oscillators, realizing amplitude death (AD) [15] in identical oscillators is another challenging task.

We report a general formulation of coupling function for chaotic oscillators that can realize both the conventional type and a mixed type of synchronization. In the conventional type synchronization, all state variables of chaotic oscillators attain one form of synchronization (say, CS or AS). In case of mixed synchronization, separate state variables attain different forms of synchronization simultaneously. An adaptive method was attempted [16] recently for achieving coexisting CS and AS in identical oscillators based on Lyapunov function stability. This method is so far restricted to numerical studies only and of limited applicability. Instead, we describe a more general and a physically realizable definition of coupling using open-plus-closed-loop (OPCL) [17] method to achieve CS and AS and, in addition, to induce AD in any response system identical or mismatched. In a recent letter [18], we reported an extension of the unidirectional OPCL coupling [17] to mismatched case with experimental evidence. Here, we add details of the unidirectional coupling and then introduce AD in identical response system. We report a transition route to synchronization that obeys a scaling law independent of any system. We further extend the theory to mutual coupling for realizing AS. The mutual OPCL coupling was proposed earlier [19] for CS only. However, AS is found restricted to inversion symmetric dynamical systems only under mutual OPCL coupling. This is similar to what was reported earlier [11,20] for AS under the conventional linear unidirectional or mutual coupling. Finally, we introduce the matrix type unidirectional coupling. Using this matrix coupling, a chaotic driver can induce different possible combinations of correlated dynamics in a response system: for example, a pair of similar state variables may develop AS, while the other pair is at CS, yet another response variable can be pushed to a resting state or AD. This matrix coupling is useful in processing industry or catalytic reaction where one may need to control concentrations of reacting chemical components in different proportions for obtaining a desired product output.

The paper is structured as follows: theory of unidirectional OPCL coupling is described in Sec. II. Numerical examples of identical oscillators showing CS, AS, and AD are discussed in Sec. II A and of mismatched case in Sec. II B. The route of transition to synchrony and its scaling behavior is described in Sec. II C. The mutual OPCL coupling is described for AS in Sec. III. In Sec. IV, the matrix coupling is presented with a numerical example. Finally, results are summarized in Sec. V.

II. OPCL COUPLING: UNIDIRECTIONAL

The unidirectional OPCL coupling was first proposed to implement CS in two identical chaotic oscillators [17] and later extended to networks of identical chaotic oscillators [21]. We extended [18] the theory to mismatched oscillators to realize CS, AS, and amplification or attenuation of chaos. The coupling function is briefly described here for the mis-

matched case: a chaotic driver is defined by $\dot{y}=f(y)+\Delta f(y)$, $y \in R^n$, where $\Delta f(y)$ contains the mismatch terms. The model of the chaotic oscillator with parameters is assumed known *a priori*. It drives another chaotic oscillator $\dot{x}=f(x), x \in R^n$ to achieve a goal dynamics $g(t)=\alpha y(t)$, where α is a constant. After coupling, the response system is given by

$$\dot{x} = f(x) + D(x,g), \tag{1}$$

where the coupling function is defined as

$$D(x,g) = \dot{g} - f(g) + \left(H - \frac{\partial f(g)}{\partial g}\right)(x-g). \tag{2}$$

$\partial f(g)/\partial g$ is the *Jacobian* of the dynamical system and H is an arbitrary constant matrix $(n \times n)$. The error signal of the coupled system is defined by $e=x-g$ when $f(x)$ can be written, using the Taylor series expansion, as

$$f(x) = f(g) + \frac{\partial f(g)}{\partial g}(x-g) + \cdots. \tag{3}$$

Keeping the first-order terms in Eq. (3) and substituting in Eq. (2), the error dynamics is obtained as $\dot{e}=He$ from Eq. (1). Now if H becomes a Hurwitz matrix whose eigenvalues all have negative real parts, $e \to 0$ as $t \to \infty$ [17,18] and we obtain asymptotically stable synchronization.

The essential of the coupling function to achieve synchronization is the appropriate selection of the elements of the H matrix that is constructed from the Jacobian of the model flow of the interacting oscillators. The elements of the matrix, H_{ij}, are chosen as $H_{ij}=(\partial f(g)/\partial g)_{ij}$ when $(\partial f(g)/\partial g)_{ij}$ is a constant in Eq. (2). If $(\partial f(g)/\partial g)_{ij}$ involves any state variable, it is replaced by a constant p_{ij}. Next essential factor in the definition of the coupling function is appropriate choice of the parameter values p_{ij}. They are to be so selected as to satisfy Routh-Hurwitz (RH) criterion [17] that ensures eigenvalues all with negative real parts. The H is then defined as a Hurwitz matrix. For a three-dimensional system, the H matrix (3×3) has the characteristic equation

$$\lambda^3 + a_1\lambda^2 + a_2\lambda + a_3 = 0, \tag{4}$$

where a_i $(i=1,2,3)$ are constants and the RH criterion is given by $a_1>0, a_1a_2>a_3, a_3>0$. Once the RH criterion for the H matrix is fulfilled, an asymptotic stability of synchronization is established even in the presence of parameter mismatch. The multiplying constant α in the goal dynamics can now be used as a control parameter to realize either of the correlated dynamics, CS $(\alpha=1)$, AS $(\alpha=-1)$, and attenuation $(0<|\alpha|<1)$ or amplification $(|\alpha|>1)$ along with AS or CS. A state of AD can also be induced in the response system by a choice of $\alpha=0$. This general form of the coupling thus allows flexibility in switching one to the other type of synchronization (AS or CS) and controlling of amplification or attenuation. This capability of switching synchronization has a potential application in message encoding [22].

A. Numerical simulation: Identical oscillators

We elaborate the unidirectional OPCL coupling in two identical oscillators using a spiking-bursting Hindmarsh-Rose (HR) neuron model [23],

$$\dot{y}_1 = y_2 - ay_1^3 + by_1^2 - y_3 + I, \quad \dot{y}_2 = c - dy_1^2 - y_2,$$

$$\dot{y}_3 = r\{s(y_1 + 1.6) - y_3\}. \tag{5}$$

y_1 is the membrane potential, y_2 and y_3 are associated with fast and slow membrane currents, and I is the bias current. The Jacobian of the model is

$$\frac{\partial f}{\partial y} = [-3ay_1^2 + 2by_1 \ 1 \ -1; \ -2dy_1 - 1 \ 0; \ rs \ 0 \ -r]^T, \tag{6}$$

where $y=[y_1 \ y_2 \ y_3]^T$; T denotes transpose of a matrix. The H matrix of the HR model is obtained from its Jacobian as explained above,

$$H = [p_1 \ 1 \ -1; \quad p_2 \ -1 \ 0; \ rs \ 0 \ -r]^T. \tag{7}$$

We consider model (5) as the driver and another identical HR system as a response. The coupling function $D(x,g)$ is then derived using Eqs. (2) and (3). The response HR oscillator after coupling is obtained as

$$\dot{x}_1 = x_2 - ax_1^3 + bx_1^2 - x_3 + I + a\alpha(\alpha^2-1)y_1^3 + b\alpha(1-\alpha)y_1^2 + (\alpha-1)I + \{p_1 - 2b\alpha y_1 + 3a(\alpha y_1)^2\}(x_1 - \alpha y_1),$$

$$\dot{x}_2 = c - dx_1^2 - x_2 + c(\alpha-1) + d\alpha(\alpha-1)y_1^2 + (p_2 + 2d\alpha y_1)(x_1 - \alpha y_1),$$

$$\dot{x}_3 = r\{s(x_1 + 1.6) - x_3\} + 1.6rs(\alpha-1). \tag{8}$$

For the H matrix in Eq. (7) to be a Hurwitz matrix, the parameters (p_1,p_2) are appropriately selected to fulfill the RH criterion, $p_1<r+1$, when we assume $p_2=0$. For our simulation, we select $p_1=-1.5$ to realize CS and AS by choosing $\alpha=1,-1$, respectively. Figure 1 shows the time series x_1 and y_1 of response and driver neurons. Plots of x_1 vs y_1 confirm CS $(\alpha=1)$ and AS $(\alpha=-1)$. For a choice of $\alpha=0$, the driver neuron can induce AD or a resting state [15] in an identical response neuron: all the response variables cease to zero amplitude although only one of the response variables, x_1, is shown in Fig. 1(e). Another option is to induce attenuation (amplification) over and above AS or CS at the response by a choice of $0<|\alpha|<1(|\alpha|>1)$. However, it is more interesting if one can control different response variables in different correlated states with those of the driver: any one of the state variables in response remains oscillatory and develops AS or CS with a similar variable of the driver and another in attenuated (amplified) state over and above in CS or AS and even may be pushed to a resting state by the driver. This opens up possibilities of controlling the level of, say, membrane voltage and slow and fast currents across the membrane of a neuron and yet maintains different forms of synchronization. This mixed type synchronization is discussed in Sec. IV in more detail.

B. Numerical simulations: Mismatched oscillators

We now describe the mismatched case with the example of Rössler system,

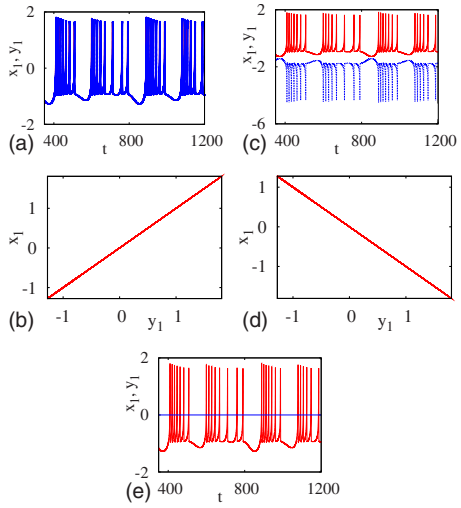

FIG. 1. (Color online) Coupled HR neuron model: $a=1.0$, $b=3.0$, $c=1.0$, $d=5.0$, $S=5.0$, $r=0.003$, $I=4.1$, and $p_1=-1.5$. Time series x_1 and y_1 in (a) and plot of x_1 vs y_1 in (b) show CS ($\alpha=1$). Time series y_1 (solid line) and x_1 (dotted line) in (c) and x_1 vs y_1 plot in (d) show AS ($\alpha=-1$). Plot of x_1 is scaled down in (c) for visual clarity. Oscillatory driver y_1 and response x_1 in horizontal zero line confirms AD ($\alpha=0$) in (e).

$$\dot{x}_1 = -\omega x_2 - x_3, \quad \dot{x}_2 = x_1 + b x_2,$$

$$\dot{x}_3 = c + x_3(x_1 - d). \tag{9}$$

The driver Rössler oscillator with mismatches is given by

$$\dot{y}_1 = -\omega y_2 - y_3 - \Delta\omega y_2, \quad \dot{y}_2 = y_1 + b y_2 + \Delta b y_2,$$

$$\dot{y}_3 = c + y_3(y_1 - d) + \Delta c - \Delta d y_3, \tag{10}$$

where $\Delta\omega$, Δb, Δc, and Δd are the mismatches in parameters. The H matrix is again obtained from the Jacobian of the Rössler model while the coupling function is defined using Eqs. (2) and (3). The response for the mismatched oscillator after coupling is

$$\dot{x}_1 = -\omega x_2 - x_3 - (\alpha\Delta\omega) y_2, \quad \dot{x}_2 = x_1 + b x_2 + (\alpha\Delta b) y_2,$$

$$\dot{x}_3 = c\alpha + x_3(x_1 - d) + \alpha\Delta c + (\alpha\Delta d) y_3 + \alpha(1-\alpha) y_1 y_3 + (p_1 - \alpha y_3)(x_1 - \alpha y_1) + (p_2 - \alpha y_1)(x_3 - \alpha y_3). \tag{11}$$

Note that the coupling in Eq. (11) has nonlinear components and, in addition, there exist linear coupling terms one for each of mismatch parameter. The linear coupling terms obviously vanish for identical $[\Delta f(y)=0]$ oscillators as shown in the first example. This linear coupling plays crucial role in the stability of synchronization. Details are presented in Sec. II C. The error dynamics is still governed by $\dot{e}=He$ and asymptotically stable for choices of parameters in H matrix to be Hurwitz. For current simulations, we choose $p_1=10$ and $p_2=-10$ from a range of possible values shown in a phase diagram in Fig. 2. It has a dark region in parameter space of (p_1,p_2) for which the H matrix has eigenvalues all with negative real parts. One can easily choose (p_1,p_2) from this phase diagram to implement CS or AS. Similar phase diagram can always be drawn for any dynamical system to allow a wider choice of parameters in H matrix to fulfill the RH criterion. Numerical results of coupled dynamics are shown in Fig. 3 for choices of $\alpha=1,-1$. Time series x_1 and y_1 are only shown here but it is also true for other pairs of state variables of the driver and the response. Note that AS is established even though the Rössler oscillator is not an inversion symmetric system. This is in contrast to the earlier [11,20] observations on antisynchronization via conventional linear coupling. This fact is further elaborated with the example of axial symmetric Lorenz system,

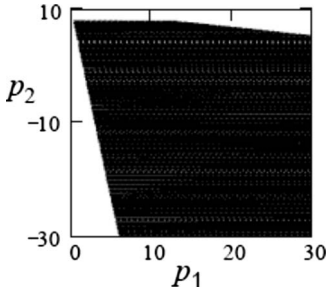

FIG. 2. Phase diagram of (p_1,p_2) in Rössler system: choice of parameters in H matrix; eigenvalues all have negative real parts in the dark region.

$$\dot{x}_1 = \sigma(x_2 - x_1), \quad \dot{x}_2 = r x_1 - x_2 - x_1 x_3,$$

$$\dot{x}_3 = -b x_3 + x_1 x_2. \tag{12}$$

The driver Lorenz system with mismatch is

$$\dot{y}_1 = (\sigma + \Delta\sigma)(y_2 - y_1),$$

$$\dot{y}_2 = (r + \Delta r) y_1 - y_2 - y_1 y_3,$$

$$\dot{y}_3 = -(b + \Delta b) y_3 + y_1 y_2, \tag{13}$$

where $\Delta\sigma$, Δr, and Δb are the mismatches. System (13) drives Eq. (12) when the coupling function is derived using

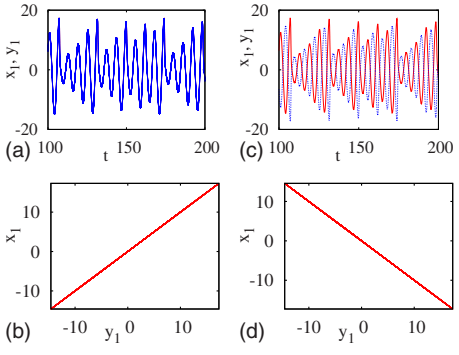

FIG. 3. (Color online) Coupled mismatched Rössler system. Response: $\omega=1$, $b=0.15$, $c=0.2$, and $d=10$; driver parameters are identical except $\Delta\omega=0.15$. Time series of x_1 and y_1 in (a) and plot of x_1 vs y_1 in (b) confirm CS for $\alpha=1$; time series of x_1 (solid line) and y_1 (dotted line) in (c) and plot of x_1 vs y_1 in (d) confirm AS. $H=|0\ -1\ -1;\ 1\ b\ 0;\ p_1\ 0\ p_2|^T$.

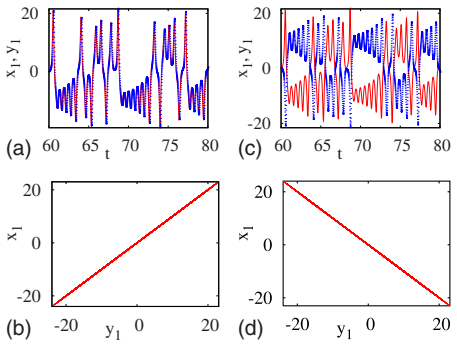

FIG. 4. (Color online) Coupled mismatched Lorenz system. Response: $r=28$, $\sigma=10$, and $b=8/3$, driver identical except $\Delta r=10$; $\varepsilon=1$. Time series of x_1 and y_1 in (a), and plot of y_1 vs x_1 in (b) confirm CS ($\alpha=1$). Time series of x_1 (solid line) and y_1 (dotted line) in (c) and plot of y_1 vs x_1 in (d) show AS ($\alpha=-1$).

Eqs. (2) and (3). The H matrix (3×3) for the Lorenz system is obtained as

$$H = |-\sigma\ \sigma\ 0;\ r+p_1\ -1\ p_2;\ p_3\ p_4\ -b|^T.$$

The response system after coupling is then derived,

$$\dot{x}_1 = \sigma(x_2 - x_1) + \alpha\Delta\sigma(y_2 - y_1),$$

$$\dot{x}_2 = rx_1 - x_2 - x_1x_3 + (\alpha\Delta r)(1/\varepsilon)y_1 + \alpha(\alpha-1)y_1y_3 + (p_1+\alpha y_3)(x_1-\alpha y_1) + (p_2+\alpha y_1)(x_3-\alpha y_3),$$

$$\dot{x}_3 = -bx_3 + x_1x_2 - (\alpha\Delta b)y_3 + \alpha(1-\alpha)y_1y_2 + (p_3-\alpha y_2)(x_1-\alpha y_1) + (p_4-\alpha y_1)(x_2-\alpha y_2). \quad (14)$$

Although the coupling appears complicated in Eq. (14), one may simplify the coupling by suitable choices of $p_k(k=1,2,3,4)$ in H matrix. A typical choice is $p_2=0$, $p_3=0$, $p_4=0$, and $p_1<1-r$ when the RH criterion is fulfilled and H becomes a Hurwitz matrix. For further reduction in coupling complexity, the driver is chosen identical to the response except that $r+\Delta r=38$ and $\Delta\sigma=0$, $\Delta b=0$. We deliberately insert a tuning parameter ε in Eq. (14) to check the role of linear coupling that appears due to a mismatch Δr. The $\varepsilon=\varepsilon_c=1$ is the critical value for asymptotic stability of synchronization. Results of numerical simulation of coupled Lorenz systems (13) and (14) are shown in Fig. 4. Plots of time series x_1 and y_1 and of y_1 vs x_1 show CS for $\alpha=1$ and AS for $\alpha=-1$. All the time series are identical in amplitude but opposite in phase for $\alpha=-1$ although only one of the state variables is shown in Fig. 4 (see Ref. [18] for details). Hence, in axial symmetric Lorenz system too, we achieve complete AS that is contrary to the existing knowledge in literature [11,20]. Thus unidirectional OPCL coupling overrules the restriction that AS can be observed in inversion symmetric system only.

Next, we present an example of a Sprott system [24] that has single quadratic nonlinearity and the coupling is much simpler for practical implementation [18]. The Sprott system is given by

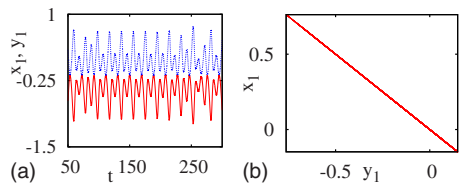

FIG. 5. (Color online) Coupled Sprott system: $a=0.225$, $\Delta a=0.025$; $p_1=-1$, $\alpha=-1$: Time series y_1 (solid line) of driver and x_1 (dotted line) of response in (a) are in AS; plot of y_1 vs x_1 in (b) also confirm AS. $H=[0\ -a\ 0;\ \ 1\ 0\ 1;\ \ 1\ p\ -1]^T$.

$$\dot{x}_1 = -ax_2, \quad \dot{x}_2 = x_1 + x_3,$$

$$\dot{x}_3 = x_1 + x_2^2 - x_3. \quad (15)$$

Another mismatch Sprott system is taken as a driver,

$$\dot{y}_1 = -ay_2 - \Delta a y_2, \quad \dot{y}_2 = y_1 + y_3,$$

$$\dot{y}_3 = y_1 + y_2^2 - y_3. \quad (16)$$

After coupling, response (15) becomes

$$\dot{x}_1 = -ax_2 - \alpha\Delta a(1/\varepsilon)y_2, \quad \dot{x}_2 = x_1 + x_3,$$

$$\dot{x}_3 = x_1 + x_2^2 - x_3 + \alpha(1-\alpha)y_2^2 + (p - 2\alpha y_2)(x_2 - \alpha y_2). \quad (17)$$

ε is again inserted as a tuning parameter and taken unity for the current simulation. The driver and the response are chaotic before coupling for $a=0.225$, $\Delta a=0.025$. For a choice of $p=-1$, H becomes a Hurwitz matrix when we find the time series of the driver and the response in AS in left panel of Fig. 5 for control parameter $\alpha=-1$. Plot of x_1 vs y_1 in the right also confirms AS. Note that all state variables are in AS with the driver variables although the system is not an inversion symmetric one.

C. Transition route to synchronization

As discussed above, the OPCL coupling has only nonlinear components for identical oscillators. Additional coupling terms appear due to parameter mismatches. The additional coupling is linear if a mismatch is attached with a linear term of the system of differential equations modeling a dynamical system as shown in the examples of Rössler system, the Lorenz oscillator, and a Sprott system. However, the additional coupling is nonlinear if the mismatch parameter is attached to a nonlinear term of the system of differential equations. The additional coupling (linear for current examples) helps neutralize the destabilization effect on synchronization due to mismatches. To explain their roles on the process of transition to synchrony, we have inserted a parameter ε in Eqs. (14) and (17) for both the Lorenz oscillator and the Sprott system, respectively. This control parameter ε is tuned from both sides of the critical value ($\varepsilon=\varepsilon_c=1$): higher and lower values as positive and negative variations in mismatch. A similarity function δ_ε is then used [1] to estimate the synchronization error between the driver and the response for varying ε,

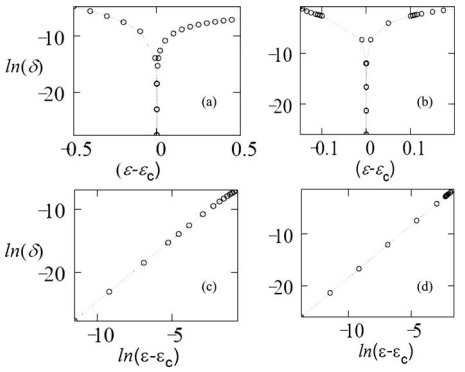

FIG. 6. Transition route to synchronization: (a) and (c) coupled Sprott system; (b) and (d) Lorenz system. Open circles for numerical data points. Slope in (b) and (d): $\gamma \sim 1.57$.

$$\delta_\varepsilon = \frac{\langle [x_1(t) - \alpha y_1(t-\tau)]^2 \rangle}{[\langle x_1(t)^2 \rangle \langle y_1(t)^2 \rangle]^{1/2}}. \tag{18}$$

The similarity function is a statistical measure of the error between two similar state variables (x_1 and y_1) of the driver and the response oscillators with an arbitrary delay τ. It is used as a standard measure of synchronization, particularly, useful in experiments [25]. For a fixed coupling strength in coupled oscillators, it shows periodic variations [1,25] for varying delay (τ) but with a global minimum $\delta_\varepsilon = \delta_{\min}$. The similarity function identifies LS when a global minimum exists at a finite value of $\tau \neq 0$. However, a global minimum, Δ
$\delta_\varepsilon = \delta_{\min} = 0$, at $\tau = 0$ can also identify CS or AS depending on the sign of α values. It needs only two similar state variables of a driver and a response to estimate the synchronization error that is advantageous in experimental conditions of limited measurement accessibility. For the Sprott system with a mismatch, $\Delta a = 0.025$, we vary ε from 0.5 to 1.5 and estimate the corresponding $\delta_{\min}(\tau=0)$ for each of ε value using numerically simulated time series (x_1 and y_1) and then plot $\ln(\delta)$ vs $(\varepsilon - \varepsilon_c)$ as shown in Fig. 6(a). The $\delta_{\min}$ has nonzero values for all ε values ($\tau=0$) except at a critical value $\varepsilon = \varepsilon_c$ when $\delta_{\min}=0$ at $\tau=0$. This is revealed as a sharp dipping of $\ln(\delta)$ into a minimum at the critical value $\varepsilon_c = 1$ when $\delta_{\min}=0(\tau=0)$, confirming synchronization. Effectively, the parameter ε acts as a strength of the additional linear coupling due to mismatch. Any compromise with the strength of the linear coupling will induce degradation in synchrony. The process of transition to synchrony with control of ε is found independent of any system and type of mismatch as we find the process to repeat for coupled Lorenz system, as shown in Fig. 6(b). For the Lorenz system, ε is varied from 0.8 to 1.2. It is interesting to note that this route of transition to synchrony follows a unique scaling law $\delta = (\varepsilon - \varepsilon_c)^\gamma$, where $\gamma \sim 1.57$ is the slope, and this scaling law is found valid for both the Sprott system and the Lorenz system as shown in Figs. 6(c) and 6(d), respectively. It is also found true for other systems such as Rössler oscillator. This remains unchanged whether it is a transition to CS or AS. If we notice Eqs. (14) and (17) carefully, we find that the coupling added a matching term in the response relating to the mismatch term in the driver. This matching term in the response is actually tuned by ε until it ensures synchronization at a critical value $\varepsilon = \varepsilon_c$ when the response becomes identical to the driver. We must mention that the definition and approach of the OPCL coupling are different from the conventional linear coupling. Under the conventional linear coupling, a bubbling transition or on-off intermittency [26] is observed near the critical coupling strength. This mismatch-induced instability in synchronization is overcome by increasing the coupling strength. In the process, PS and LS are observed in mismatch oscillators with increasing coupling strength and an almost CS state is finally obtained for very strong coupling. However, the coupled oscillators remain mismatched even after the synchronization is achieved. On the other hand, in OPCL coupling, the coupled oscillators become identical once synchronization is established at a critical value of $\varepsilon = \varepsilon_c$. This is a mark difference in the process of synchronization under the OPCL coupling and the conventional linear coupling. We have also checked that no on-off intermittency is observed near the $\varepsilon = \varepsilon_c$, higher or lower. Thus the OPCL coupling has inherent capability to take care of the mismatch in coupled oscillators and to provide immunity to stable synchronization by tuning the control parameter ε. The capability of such a tuning of the control parameter (ε) can be used for parameter estimation.

III. OPCL METHOD: MUTUAL COUPLING

The OPCL coupling in mutually interacting chaotic oscillators was investigated [19] earlier to realize CS, but AS was not studied there. Now we extend the theory of mutual OPCL coupling to AS. Two mutually interacting oscillators under OPCL coupling are

$$\dot{x} = f(x) + D_x(x,y), \quad x \in R^n,$$

$$\dot{y} = f(y) + D_y(x,y), \quad y \in R^n, \tag{19}$$

where the coupling terms are defined by

$$D_x(x,y) = \left(H - \left. \frac{df}{dx} \right|_{x=s_+} \right) \left(\frac{x-y}{2} \right) \tag{20}$$

and

$$D_y(x,y) = \left(H - \left. \frac{df}{dy} \right|_{y=s_+} \right) \left(\frac{y-x}{2} \right), \tag{21}$$

where $s_+(t) = (x(t) + y(t)/2)$ is the synchronization manifold. It can be easily established that the error dynamics is governed by $\dot{e} = He$ and its zero error solution or synchronization is asymptotically stable once H is a Hurwitz matrix by an appropriate selection of its parameters so as to satisfy the RH criterion. Numerical results are presented in detail in Ref. [19]. To realize AS using mutual coupling, we modify the coupling in Eqs. (20) and (21) to Eqs. (22) and (23), respectively,

$$D_x(x,y) = \left(H - \left. \frac{df}{dx} \right|_{x=s_-} \right) \left(\frac{x+y}{2} \right) \tag{22}$$

and

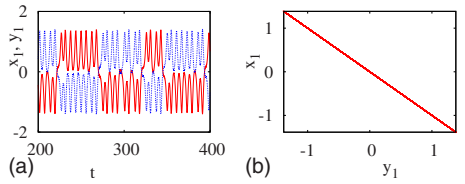

FIG. 7. (Color online) Antisynchronization for mutual coupling in double scroll system: $c=0.436$, $p=-1.5$. Time series x_1 (solid line) and y_1 (dotted line) of the coupled oscillators in (a) and y_1 vs x_1 plot in (b) confirms AS. $H=[0\ c\ -1;\ 1\ -1\ 0;\ p\ -1\ 0]^T$.

$$D_y(x,y)=\left(H-\left.\frac{df}{dy}\right|_{x=s_-}\right)\left(\frac{x+y}{2}\right), \tag{23}$$

where $s_-(t)=(x(t)-y(t)/2)$ is the antisynchronization manifold. However, for AS, an additional condition of inversion symmetry of the flow of a model system $f(y)=-f(-y)[f(x)=-f(-x)]$ is necessary to be satisfied. Then only the error dynamics can follow $\dot{e}=He$ when the error state is $e=(x+y)$ for AS, and it is asymptotically stable provided H is a Hurwitz matrix. As mentioned above, such a restriction of inversion symmetry of a dynamical system always exists for AS under linear mutual or unidirectional coupling [11,20], while it is overruled in case of unidirectional OPCL coupling. For numerical demonstration, we take an inversion symmetric double scroll system [27] that is defined by

$$\dot{x}_1=cx_1+x_3,\quad \dot{x}_2=x_1-x_2,\quad \dot{x}_3=x_1^3-x_2. \tag{24}$$

The system has single cubic nonlinearity and shows one-scroll or two-scroll chaos [27] with appropriate choice of parameter. After the mutual OPCL coupling is established, the coupled double scroll system is obtained as

$$\dot{x}_1=cx_1+x_3,\quad \dot{x}_2=x_1-x_2,$$

$$\dot{x}_3=x_1^3-x_2+\left(p+3\frac{(x_1-y_1)^2}{4}\right)\frac{(x_1+y_1)}{2},$$

$$\dot{y}_1=cy_1+y_3,\quad \dot{y}_2=y_1-y_2,$$

$$\dot{y}_3=y_1^3-y_2+\left(p+3\frac{(y_1-x_1)^2}{4}\right)\frac{(x_1+y_1)}{2}. \tag{25}$$

Numerical results of AS in double scroll systems are shown in Fig. 7. Time series of the coupled oscillator x_1 and y_1 and plot of y_1 vs x_1 confirm AS.

IV. OPCL COUPLING: MATRIX TYPE

Now we introduce the matrix type OPCL coupling. We remind that for synchronization using unidirectional coupling, we set a goal dynamics $g(t)=\alpha y(t)$ in Eq. (1), where $y(t)=[y_1\ y_2\ y_3]^T$ is the driver state and α is a constant. As a result, all state variables of the response system are forced into either a CS or AS state with the driver variables as decided by a choice of the α value. Even AD can be induced to a response system by a choice of $\alpha=0$. We generalize this result to achieve CS, AS, and AD simultaneously in different state variables by defining a new goal dynamics $\tilde{g}(t)$,

$$\tilde{g}(t)\overset{\Delta}{=}[g_1(t)\ g_2(t)\ g_3(t)]^T=[\alpha_1 y_1\ \alpha_2 y_2\ \alpha_3 y_3]^T, \tag{26}$$

where α_i $(i=1,2,3)$ is again a constant. The response system after coupling becomes

$$\dot{x}=f(x)+D(x,\tilde{g}), \tag{27}$$

where the coupling function is defined by

$$D(x,\tilde{g})=\begin{bmatrix}\alpha_1\dot{y}_1\\ \alpha_2\dot{y}_2\\ \alpha_3\dot{y}_3\end{bmatrix}-f(\tilde{g})+\left(H-\frac{\partial f(\tilde{g})}{\partial(\tilde{g})}\right)\begin{bmatrix}x_1-\alpha_1 y_1\\ x_2-\alpha_2 y_2\\ x_3-\alpha_3 y_3\end{bmatrix}. \tag{28}$$

The rest of the theory is similar to what is presented in Sec. II and can be easily derived. Note that Eq. (28) is a general form of Eq. (2) for unidirectional OPCL coupling; if $\alpha_1=\alpha_2=\alpha_3$ is considered, Eq. (2) is restored from Eq. (28) for two identical oscillators $[\Delta f(y)=0]$. For illustration, we consider the example of Sprott system (15). The response and driver systems are assumed identical before coupling and hence the models remain unchanged as in Eqs. (15) and (16), respectively, except that the mismatch in Eq. (16) vanishes $(\Delta a=0)$. After matrix coupling, the response becomes

$$\dot{x}_1=-ax_2+a(\alpha_2-\alpha_1)y_2,$$

$$\dot{x}_2=x_1+x_3+(\alpha_2-\alpha_1)y_1+(\alpha_2-\alpha_3)y_3,$$

$$\dot{x}_3=x_1+x_2^2-x_3+(\alpha_3-\alpha_2^2)y_2^2+(p-2\alpha_2 y_2)(x_2-\alpha_2 y_2)+(\alpha_3-\alpha_1)y_1. \tag{29}$$

Matrix coupling thus allows choices of different goals set by α_i for different state variables of a response system, as shown in Fig. 8. AS state is realized in one response variable when CS in the other and AD in another response variable. Similarly, partial attenuation and/or amplification can also be induced by appropriate choice of the α_i values. As mentioned above, the matrix coupling appears interesting from a practical viewpoint: in processing industry, concentration of any of the constituents of a reaction system can either be reduced or enhanced and even made zero. In neuron oscillators too, one can switch off any state variable as membrane voltage while reducing other membrane current for achieving a desired neural dynamics. The results can be easily extended to mismatched systems that we do not elaborate here.

V. SUMMARY

A general formulation of coupling function is presented, which is capable of targeting desired responses such as CS, AS, and AD in identical as well as mismatched chaotic oscillators. The coupling function is defined for three different coupling schemes, unidirectional, mutual, and matrix type coupling, which are all based on Hurwitz matrix stability. The Hurwitz matrix can be derived from the Jacobian of the

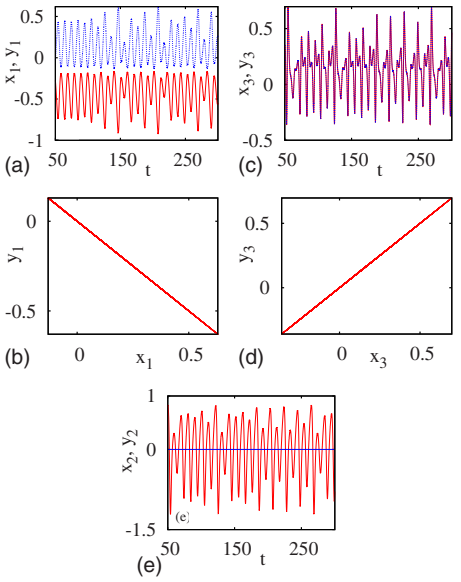

FIG. 8. (Color online) Mixed synchronization in Sprott system: $a=0.225$. Time series y_1 (solid line) of driver and x_1 (dotted line) of response in (a) and plot of y_1 vs x_1 in (b) confirm AS for ($\alpha_1=-1$). Time series of y_3 and x_3 in (c) and plot of y_3 vs x_3 in (d) shows CS for $\alpha_3=1$. Steady state response or AD of response x_2 is shown as horizontal line at zero while y_2 of chaotic driver remain oscillatory for $\alpha_2=0$ in (e).

model flow of a dynamical system. The success of the coupling in inducing asymptotically stable synchronization depends on appropriate selection of parameters of the Hurwitz matrix. An additional parameter is introduced in the coupling function that can control CS or AS and thereby allows switching between CS and AS states for practical purposes [22]. A numerical example of spiking-bursting Hindmarsh-Rose neuron model is presented to illustrate the coupling for two identical oscillators. It is demonstrated that even cessation of oscillation or AD can be induced in an identical response system. Since in reality no two systems are identical, we extended the coupling function for mismatched chaotic systems. We find an interesting scaling behavior that appears during the process of transition to synchrony when one tunes a coupling parameter in the coupled system. We further extended the results to mutual OPCL coupling to realize AS in chaotic systems and infer that AS is so far possible in inversion symmetric systems only under mutual OPCL coupling. Finally, we introduce a matrix type unidirectional OPCL coupling by which it is possible to induce AS, CS, and even AD simultaneously in different state variables of a response system. This has potential application in processing industry if one intends to enhance or to reduce the concentration and even remove another component in catalytic reactions to obtain a desired final product. The OPCL coupling is also able to realize AS and AD in two dynamical network results of which are reported elsewhere [28]. We conclude that although the mathematical formulation looks complicated, the coupling is still physically realizable as shown earlier [18] and may be used for practical purposes [22].

ACKNOWLEDGMENTS

This work was supported by the Ministry of Education and Research, Romania and the Ministry of Science & Technology, India. I.G. acknowledges support from FUNCDYN program of ESF and Grants No. 12115/2008 and No. 2219/2009 from CNCSIS, Romania. S.K.D. acknowledges partial support by the DST, India under Grant No. SR/S2/HEP-03/2005. R.B. acknowledges support of the CSIR, India.

[1] A. S. Pikovsky, M. G. Roseblum, and J. Kurths, *Synchronization: A Concept in Nonlinear Sciences* (CUP, New York, 2001); S. Boccaletti, J. Kurths, G. Osipov, D. L. Valladares, and C. Zhou, Phys. Rep. **366**, 1 (2002).

[2] *Complex Dynamics in Physiological Systems: From Heart to Brain*, Complexity Series, edited by S. K. Dana, P. K. Roy, and J. Kurths (Springer, New York, 2009).

[3] P. J. Uhlhaas and W. Singer, Neuron **52**, 155 (2006).

[4] A. Argyris, D. Syvridis, L. Larger, V. Annovazzi-Lodi, P. Colet, I. Fischer, J. García-Ojalvo, C. R. Mirasso, L. Pesquera, and K. A. Shore, Nature (London) **438**, 343 (2005).

[5] V. In, A. R. Bulsara, A. Palacios, P. Longhini, A. Kho, and J. D. Neff, Phys. Rev. E **68**, 045102(R) (2003); A. R. Bulsara *et al.*, Phys. Lett. A **353**, 4 (2006); P. Longhini, A. Palacios, V. In, J. D. Neff, A. Kho, and A. Bulsara, Phys. Rev. E **76**, 026201 (2007).

[6] M. G. Rosenblum and A. S. Pikovsky, Phys. Rev. Lett. **92**, 114102 (2004); J. Mayer, H. G. Schuster, J. C. Claussen, and M. Mölle, *ibid.* **99**, 068102 (2007); D. Contreras, A. Destexhe, T. J. Sejnowski, and M. Steriade, Science **274**, 771 (1996).

[7] O. V. Popovych, C. Hauptmann, and P. A. Tass, Phys. Rev. Lett. **94**, 164102 (2005).

[8] V. N. Belykh, G. V. Osipov, N. Kucklander, B. Blasius, and J. Kurths, Physica D **200**, 81 (2004).

[9] I. Z. Kiss, C. G. Rusin, H. Kori, and J. L. Hudson, Science **316**, 1886 (2007); W. L. Kath and J. M. Ottino, *ibid.* **316**, 1857 (2007).

[10] L. Pecora and T. Carroll, Phys. Rev. Lett. **64**, 821 (1990).

[11] L.-Y. Cao and Y.-C. Lai, Phys. Rev. E **58**, 382 (1998); V. Astakhov, A. Shabunin, and V. Anishchenko, Int. J. Bifurcation Chaos Appl. Sci. Eng. **10**, 849 (2000); W. Liu, J. Xiao, X. Qian, and J. Yang, Phys. Rev. E **73**, 057203 (2006); C.-M. Kim, S. Rim, W.-H. Kye, J. W. Ryu, and Y.-J. Park, Phys. Lett. A **320**, 39 (2003).

[12] M. G. Rosenblum, A. S. Pikovsky, and J. Kurths, Phys. Rev. Lett. **76**, 1804 (1996); **78**, 4193 (1997).

[13] N. F. Rulkov, M. M. Suschik, L. S. Tsimring, and H. D. I. Abarbanel, Phys. Rev. E **51**, 980 (1995); H. D. I. Abarbanel, N. F. Rulkov, and M. M. Sushchik, *ibid.* **53**, 4528 (1996).

[14] A. E. Hramov and A. A. Koronovskii, Chaos **14**, 603 (2004); Physica D **206**, 252 (2005); A. E. Hramov, A. A. Koronovskii, M. K. Kurovskaya, and O. I. Moskalenko, Phys. Rev. E **71**,

056204 (2005).
[15] D. G. Aronson, G. B. Ermentrout, and N. Kopell, Physica D **41**, 403 (1990); S. H. Strogatz, Nature (London) **394**, 316 (1998); D. V. Ramana Reddy, A. Sen, and G. L. Johnston, Phys. Rev. Lett. **80**, 5109 (1998); A. Prasad, J. Kurths, S. K. Dana, and R. Ramaswamy, Phys. Rev. E **74**, 035204(R) (2006); R. Karnatak, R. Ramaswamy, and A. Prasad, *ibid.* **76**, 035201(R) (2007).
[16] C. Li, Q. Chen, and T. Huang, Chaos, Solitons Fractals **38**, 461 (2008).
[17] E. A. Jackson and I. Grosu, Physica D **85**, 1 (1995); I. Grosu, Phys. Rev. E **56**, 3709 (1997); Int. J. Bifurcation Chaos Appl. Sci. Eng. **17**, 3519 (2007).
[18] I. Grosu, E. Padmanaban, P. K. Roy, and S. K. Dana, Phys. Rev. Lett. **100**, 234102 (2008).
[19] A. I. Lerescu, S. Oancea, and I. Grosu, Phys. Lett. A **352**, 222 (2006).
[20] V. Belykh, I. Belykh, and M. Hasler, Phys. Rev. E **62**, 6332 (2000).
[21] C. Li, W. Sun, and J. Kurths, Phys. Rev. E **76**, 046204 (2007).
[22] E. Padmanaban, I. Grosu, and S. K. Dana (unpublished).
[23] J. L. Hindmarsh and R. M. Rose, Proc. R. Soc. London, Ser. B **221**, 87 (1984).
[24] J. C. Sprott, Phys. Rev. E **50**, R647 (1994).
[25] P. K. Roy, S. Chakraborty, and S. K. Dana, Chaos **13**, 342 (2003).
[26] P. Ashwin, J. Buescu, and I. Stewart, Phys. Lett. A **193**, 126 (1994); S. C. Venkataramani, B. R. Hunt, E. Ott, D. J. Gauthier, and J. C. Bienfang, Phys. Rev. Lett. **77**, 5361 (1996); S. C. Venkataramani, B. R. Hunt, and E. Ott, Phys. Rev. E **54**, 1346 (1996).
[27] P. K. Roy, T. K. Mukherjee, and S. K. Dana, Proceedings of the Fourth NCNSD, India, 2008; R. Thomas and M. Kaufman, Chaos **11**, 170 (2001).
[28] R. Banerjee, I. Grosu, and S. K. Dana, *Proceedings of Complex (LNICST 4)*, Computer Science Series (Springer, New York, 2009), Pt. I, pp. 1072–1082.